J|A|C|S ARTICLES

Published on Web 02/26/2010

Fluoride Rearrangement Reactions of Polyphenyl- and Polyvinylsilsesquioxanes as a Facile Route to Mixed Functional Phenyl, Vinyl T_{10} and T_{12} Silsesquioxanes

M. Z. Asuncion[†] and R. M. Laine*[,†,‡]

Departments of Macromolecular Science and Engineering and Materials Science and Engineering, University of Michigan, Ann Arbor, Michigan 48109-2136

Received October 28, 2009; E-mail: talsdad@umich.edu

Abstract: Polyphenylsilsesquioxane $[PhSiO_{1.5}]_n$ (PPS) and polyvinylsilsesquioxane $[vinylSiO_{1.5}]_n$ (PVS) are polymeric byproducts of the syntheses of the related T_8 octamers $[PhSiO_{1.5}]_8$ and $[vinylSiO_{1.5}]_8$. Here we demonstrate that random-structured PPS and PVS rearrange in the presence of catalytic amounts of $Bu_4N^+F^-$ in THF to form mixed-functionality polyhedral T_{10} and T_{12} silsesquioxane (SQ) cages in 80−90% yields. Through control of the initial ratio of starting materials, we can statistically tailor the average values for x for the $vinyl_xPh_{10-x}T_{10}$ and $vinyl_xPh_{12-x}T_{12}$ products. Metathetical coupling of $x \approx 2$ vinyl cages with 4-bromostyrene produces SQs with an average of two 4-bromostyrenyl substituents. These products can be reacted via Heck coupling with $vinylSi(OEt)_3$ to produce SQs with $vinylSi(OEt)_3$ end-caps. Alternately, Heck coupling with the originally produced $x \approx 2$ vinyl SQs leads to "beads on a chain" SQ oligomers joined by conjugated organic tethers. The functionalized T_{10} and T_{12} cages, metathesis, and Heck compounds were characterized by standard analytical methods (MALDI-TOF MS, ^1H and ^{13}C NMR spectroscopy, TGA, and GPC). MALDI confirms the elaboration of the cages after each synthetic step, and GPC verifies the presence of higher molecular weight SQ oligomers. TGA shows that all of these compounds are thermally stable in air (>300 °C). The UV−vis absorption and emission behavior of the Heck oligomers reveals exceptional red-shifts (≥60 nm) compared to the $vinylSi(OEt)_3$ end-capped model compounds, suggesting electronic interactions through the SQ silica cores. Such phenomena may imply 3-D conjugation through the cores themselves.

1. Introduction

Polyhedral silsesquioxanes, in particular the T_8 octasilsesquioxane "SQs" $[(RSiO_{1.5})_8$, Figure 1a], represent a versatile class of highly symmetrical three-dimensional organosilicon compounds with well-defined nanometer-size structures. The combination of a rigid silica core and a more flexible, modifiable organic shell makes these compounds extremely useful as platforms for assembling hybrid nanocomposite materials with properties intermediate between those of ceramics and organics.[1−12]

SQs have been used in recent years to (1) model catalytic surfaces,[13,14] (2) generate new catalysts[15] and (3) novel porous media,[16] and serve as (4) NMR standards[17] and (5) encapsulants.[18] The decameric T_{10} and dodecameric T_{12} SQs (Figure 1b,c) are frequently formed alongside the T_8 cube,[19,20] albeit in lower yields, and their derivatives often exhibit chemical,

[†] Macromolecular Science and Engineering.
[‡] Materials Science and Engineering.

(1) (a) *Organic/Inorganic Hybrid Materials*; Laine, R. M., Sanchez, C., Brinker, C. J., Giannelis, E., Eds.; MRS Symposium Series *519*; Materials Research Society: Warrendale, PA, 1998. (b) *Organic/Inorganic Hybrid Materials II*; Klein, L. C., Francis, L., DeGuire, M. R., Mark, J. E., Eds.; MRS Symposium Series *576*; Materials Research Society: Warrendale, PA, 1999. (c) *Organic/Inorganic Hybrid Materials*; Laine, R. M., Sanchez, C., Giannelis, E., Brinker, C. J., Eds.; MRS Symposium Series *628*; Materials Research Society: Warrendale, PA, 2000. (d) *Organic/Inorganic Hybrid Materials*; Laine, R. M., Sanchez, C., Yang, S., Brinker, C. J., Eds.; MRS Symposium Series *726*; Materials Research Society: Warrendale, PA, 2002. (e) Sanchez, C.; Soler-Illia, G. J.; de, A. A.; Ribot, F.; Lalot, T.; Mayer, C. R.; Cabuil, V. *Chem. Mater.* **2001**, *13*, 3061, and references therein.
(2) Sellinger, A.; Laine, R. M. *Macromolecules* **1996**, *29*, 2327.
(3) Sellinger, A.; Laine, R. M. *Chem. Mater.* **1996**, *8*, 1592.
(4) Lichtenhan, J. D.; Otonari, Y. A.; Carr, M. J. *Macromolecules* **1995**, *28*, 8435.
(5) Feher, F. J.; Budzichowski, T. A. *J. Organomet. Chem.* **1989**, *379*, 33.
(6) Feher, F. J.; Soulivong, D.; Eklud, A. G.; Wyndham, K. D. *Chem. Commun.* **1997**, 1185.
(7) Jeon, H. G.; Mather, P. T.; Haddad, T. S. *Polym. Int.* **2000**, *49*, 453.
(8) (a) Gilman, J. W.; Schlitzere, D. S.; Lichtenhan, J. D. *J. Appl. Polym. Sci.* **1996**, *60*, 591. (b) Gonzalez, R. I.; Phillips, S. H.; Hoflund, G. B. *J. Spacecraft Rockets* **2000B**, *37*, 463.
(9) Sellinger, A.; Laine, R. M.; Chu, V.; Viney, C. *J. Polym. Sci., Part A: Polym. Chem.* **1994**, *2*, 3069.
(10) Zhang, C.; Babonneau, F.; Bonhomme, C.; Laine, R. M.; Soles, C. L.; Hristov, H. A.; Yee, A. F. *J. Am. Chem. Soc.* **1998**, *120*, 8380.
(11) (a) Laine, R. M.; Choi, J.; Lee, I. *Adv. Mater.* **2001**, *13*, 800. (b) Brick, C. M.; Chan, E. R.; Glotzer, S. C.; Marchal, J. C.; Martin, D. C.; Laine, R. M. *Adv. Mater.* **2007**, *19*, 82. (c) Laine, R. M.; Zhang, C.; Sellinger, A.; Viculis, L. *Appl. Organomet. Chem.* **1998**, *12*, 715. (d) Tamaki, R.; Choi, J.; Laine, R. M. *Chem. Mater.* **2003**, *15*, 793. (e) Choi, J.; Kim, S. G.; Laine, R. M. *Macromolecules* **2004**, *37*, 99. (f) Sulaiman, S.; Brick, C. M.; De Sana, C. M.; Katzenstein, J. M.; Laine, R. M.; Basheer, R. A. *Macromolecules* **2006**, *39*, 5167.
(12) Zhang, C.; Laine, R. M. *J. Am. Chem. Soc.* **2000**, *122*, 6979.
(13) Feher, F. J.; Newman, D. A.; Walzer, J. F. *J. Am. Chem. Soc.* **1989**, *111*, 1741.
(14) (a) Feher, F. J.; Budzichowski, T. A.; Blanski, R. L.; Weller, K. J.; Ziller, J. W. *Organometallics* **1991**, *10*, 2526. (b) Feher, F. J.; Soulivong, D.; Eklud, A. G.; Wyndham, K. D. *Chem. Commun.* **1997**, *13*, 1185.

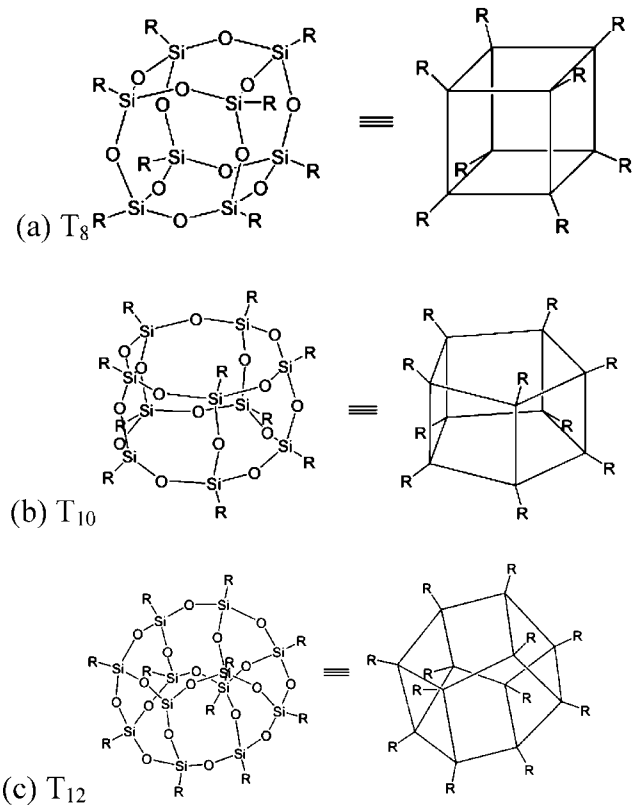

Figure 1. Idealized structures of (a) T_8 octaSQ "cube", (b) T_{10} decaSQ, and (c) T_{12} dodecaSQ.

thermal, and mechanical properties that parallel those of the T_8 derivatives.[11f,19b]

Cubic or T_8 SQs are typically prepared via acid- or base-catalyzed hydrolytic condensation of trifunctional organosilanes or by chemical transformation of pendant groups on pre-existing cages. Since their initial discovery in 1946,[21] there have been numerous studies on the synthesis of polyhedral SQs. However, no universal preparative procedures have been established, for reasons mentioned below.[19]

Many factors are known to influence the formation (and hence structure) of SQs from the hydrolytic condensation of $RSiX_3$ (where X is typically a halogen or alkoxy group): the nature of the R group, nature of the X group, solvent, concentration of

Scheme 1. Synthesis of (a) $F^-@(PhSiO_{1.5})_8$ from Reaction of Phenyltriethoxysilane and TBAF[18] and (b) $F^-@(RSiO_{1.5})_8$ by Reaction of $(RSiO_{1.5})_8$ and TMAF[27]

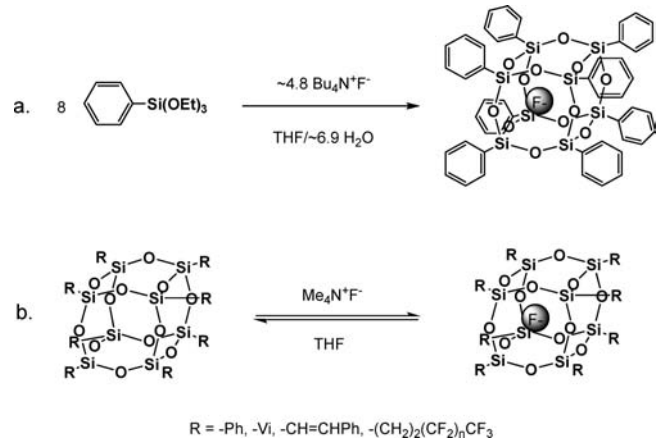

starting materials, reaction time, rate of addition and quantity of H_2O, pH, solubility of product, etc.[20] It has proven difficult to quantify the effects of these factors, either individually or collectively, because each reaction appears to be uniquely sensitive to a combination of many (if not all) of the above variables.

One common observation is that acid-catalyzed hydrolysis of trialkoxysilanes often forms T_8 SQs very slowly and with poor yields (5−30%), depending on the nature of the starting silane.[22−24] In contrast, base-catalyzed conditions generally improve reaction times and yields,[25,26] but the use of excessively strong base can also lead to undesired cage scission. Among base-promoted syntheses, Bassindale et al.[18,25] recently used F^- to promote formation of T_8 SQs from the corresponding trialkoxy compounds. They also found that F^- can be encapsulated within the SQ. Mabry, Bowers, et al.[27] recently reported a second route to SQ encapsulated F^- (see below). F^- is also known to effect rapid gelation of $Si(OEt)_4$ under sol−gel processing conditions at 25 °C.[28] In these studies tetra-*n*-butylammonium fluoride (nBu_4NF or TBAF)[18,25,27] and KF[26] were used because their solutions are only slightly basic (pK_a ~3.20 in H_2O).

The Bassindale[18] studies demonstrate direct encapsulation of F^- (octaphenylSQ or OPS; Scheme 1a) simply by careful removal of solvent following hydrolysis of phenyltriethoxysilane with stoichiometric TBAF. The structure was confirmed by ^{29}Si NMR and single-crystal X-ray diffraction (XRD). The syntheses of $F^-@(vinylSiO_{1.5})_8$ and $F^-@(p\text{-}tolylSiO_{1.5})_8$ were also reported.[18] The trapped F^- results in only very slight changes in the Si−O distances and cage bond angles from structures where the central fluoride is absent.[18,26] ^{19}F NMR shows a single, sharp

(15) (a) Feher, F. J.; Blanski, R. L. *J. Am. Chem. Soc.* **1992**, *114*, 5886. (b) Severn, J. R.; Duchateau, R.; van Santen, R. A.; Ellis, D. D.; Spek, A. L. *Organometallics* **2002**, *1*, 4. (c) Duchateau, R.; Abbenhuis, H. C. L.; van Santen, R. A.; Meetsma, A.; Thiele, S.K.-H.; van Tol, M. F. H. *Organometallics* **1998**, *26*, 5663. (d) Hanssen, R. W. J. M.; van Santen, R. A.; Abbenhuis, H. C. L. *Eur. J. Inorg. Chem.* **2004**, *4*, 675.
(16) Maxim, N.; Magusin, P. C. M. M.; Kooyman, P. J.; van Wolput, J. H. M. C.; van Santen, R. A.; Abbenhuis, H. C. L. *Chem. Mater.* **2001**, *13*, 2958.
(17) Bonhomme, C.; Toledano, P.; Maquet, J.; Livage, J.; Bohnomme-Coury, L. *J. Chem. Soc., Dalton Trans.* **1997**, *9*, 1617.
(18) (a) Bassindale, A. R.; Pourny, M.; Taylor, P. G.; Hursthouse, M. B.; Light, M. E. *Angew. Chem., Int. Ed.* **2003**, *42*, 3488. (b) Bassindale, A. R.; Parker, D. J.; Pourny, M.; Taylor, P. G.; Horton, P. N.; Hursthouse, M. B. *Organometallics* **2004**, *23*, 4400.
(19) (a) Pescarmona, P. P.; Maschmeyer, T. *J. Aust. Chem.* **2001**, *54*, 583. (b) Lickiss, P. D.; Rataboul, F. In *Advances in Organometallic Chemistry, Vol. 57*; Hill, A. F., Fink, M. J., Gordon, F., Eds.; Academic Press: United Kingdom, 2008; pp 1−116.
(20) Voronkov, M. G.; Lavrent'yev, V. I. *Top. Curr. Chem.* **1982**, *102*, 199.
(21) Scott, D. W. *J. Am. Chem. Soc.* **1946**, *68*, 356.
(22) Brown, J. F. *J. Am. Chem. Soc.* **1965**, *87*, 4317.
(23) Sprung, M. M.; Guenther, F. O. *J. Am. Chem. Soc.* **1955**, *77*, 3996.
(24) Braunstein, P.; Galsworthy, J. R.; Hendan, B. J.; Marsmann, H. C. *J. Organomet. Chem.* **1998**, *551*, 125.
(25) Bassindale, A. R.; Liu, Z.; MacKinnon, I. A.; Taylor, P. G.; Yang, Y.; Light, M. E.; Horton, P. N.; Hursthouse, M. B. *Dalton Trans.* **2003**, *14*, 2945.
(26) Koželj, M.; Orel, B. *Dalton Trans.* **2008**, *37*, 5072.
(27) (a) Anderson, S. E.; Bodzin, D. J.; Haddad, T. S.; Boatz, J. A.; Mabry, J. M.; Mitchell, C.; Bowers, M. T. *Chem. Mater.* **2008**, *20*, 4299. (b) Anderson, S. E.; Shammel Baker, E.; Mitchell, C.; Haddad, T. S.; Bowers, M. T. *Chem. Mater.* **2005**, *17*, 2537. (c) Anderson, S. E.; Mitchell, C.; Haddad, T. S.; Vij, A.; Schwab, J. J.; Bowers, M. T. *Chem. Mater.* **2006**, *18*, 1490.
(28) Pope, E. J. A.; Mackenzie, J. D. *J. Non-Cryst. Solids* **1986**, *87*, 185.

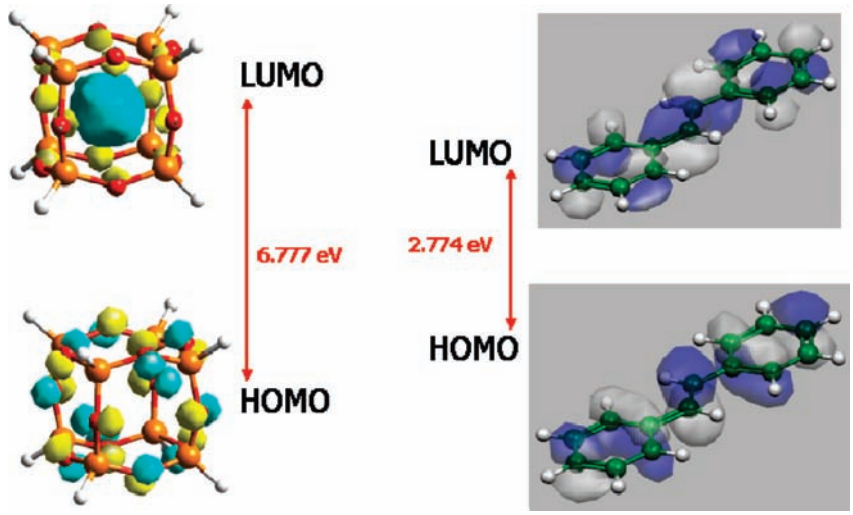

Figure 2. (a) HOMO and (b) LUMO of $[HSiO_{1.5}]_8$ and of *trans*-stilbene.[34]

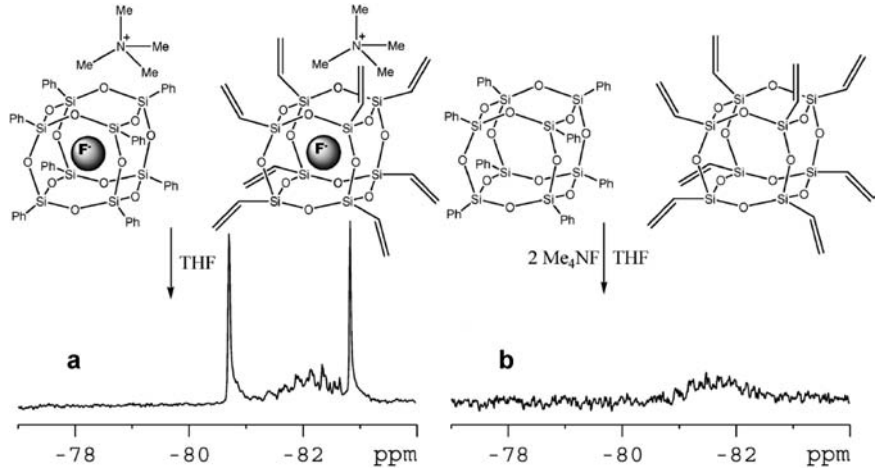

Figure 3. ^{29}Si NMR spectra obtained by mixing (a) F^-@OPS and F^-@OVS in THF and (b) TMAF with equivalent amounts of OPS and OVS in THF.[26] Adapted from ref 27a.

peak at $\delta = -26.4$ ppm, where F^- essentially behaves as a naked ion with very little coordination to the silicon atoms.[18]

Building on this work, Bowers et al.[27] synthesized a new series of F^- encapsulated cubes (for reasons discussed further below), $F^-@(RSiO_{1.5})_8$, where R = vinyl, phenyl, styrenyl, trifluoropropyl, nonafluorohexyl, or tridecafluorooctyl, by reaction of Me_4NF (TMAF) and the corresponding R_8T_8 cage (Scheme 1b).[27] While they reported that the synthesis works well for electron-withdrawing substituents, they found that it fails when R is an electron-donating group (R = ethyl, cyclohexyl, and isobutyl).

Modeling studies of $(RSiO_{1.5})_8$ (R = H, F, HO, NH_2, alkyl, etc.) by multiple groups[29−33] find that the $(RSiO_{1.5})_8$ HOMO involves the 2p lone-pair states on the oxygen atoms and lies on the edges of the cubes (Figure 2a). Those studies also find that the LUMO involves contributions from all Si and oxygen atoms and the R substituents, is spherical, and resides in the cube center (Figure 2b).[29−33] Bassindale has suggested that fluoride interaction with an electrophilic LUMO may account for the stability of F^- encapsulated silsesquioxanes.[18] Furthermore, the presence of an electronically accessible "core" state may also explain the unique red-shifted emission behavior of silsesquioxanes, as discussed further below.

While the mechanism of fluoride inclusion is uncertain, it is clearly much more complicated than a simple insertion through the cube face. Figure 3a shows the ^{29}Si NMR spectra of F^- encapsulated in OPS and octavinylsilsesquioxane (OVS) after mixing with THF.[27a] The sharp peaks at ~ -81 and ~ -83 ppm correlate to the eight equivalent silicon atoms in F^-@OPS and F^-@OVS, respectively. The numerous small peaks between the peaks of the pure starting materials suggest that many compounds with mixed phenyl and vinyl groups are generated in solution after mixing.

(29) (a) Ossadnik, C.; Veprek, S.; Marsmann, H. C.; Rikowski, E. *Monatsch. Chem.* **1999**, *130*, 55. (b) Schneider, K. S.; Zhang, Z.; Banaszak-Holl, M. M.; Orr, B. G.; Pernisz, U. C. *Phys. Rev. Lett.* **2000**, *85*, 602.
(30) Azinovic, D.; Cai, J.; Eggs, C.; Konig, H.; Marsmann, H. C.; Veprek, S. *J. Lumin.* **2002**, *97*, 40.
(31) (a) Xiang, K.-H.; Pandey, R.; Pernisz, U. C.; Freeman, C. *J. Phys. Chem. B* **1998**, *102*, 8704. (b) Cheng, W.-D.; Xiang, K.-H.; Pandey, R.; Pernisz, U. C. *J. Phys. Chem. B* **2000**, *104*, 6737.
(32) Lin, T.; He, C.; Xiao, Y. *J. Phys. Chem. B* **2003**, *107*, 13788.
(33) Laine, R. M.; Sulaiman, S.; Brick, C. M.; Roll, M. F.; Tamaki, R.; Asuncion, M. Z.; Neurock, M.; Filhol, J.-S.; Lee, C.-Y.; Goodson, T.; Ronchi, M.; Pizzotti, M.; Rand, S. C.; Li, Y. *J. Am. Chem. Soc.* **2010**; doi: 10.1021/ja9087709(accompanying paper).
(34) Ronchi, M.; Sulaiman, S.; Boston, N. R.; Laine, R. M. *Appl. Organomet. Chem.* **2010**, special issue, in press.

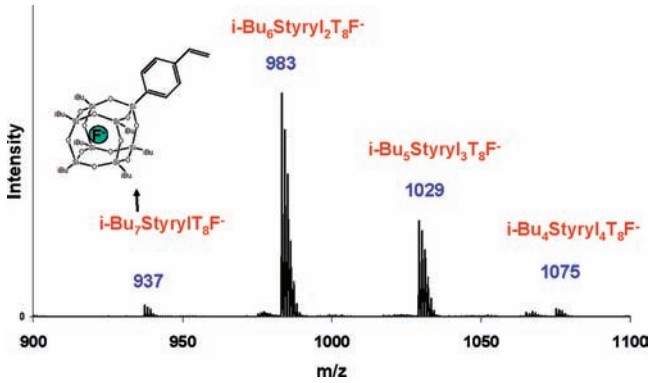

Figure 4. ESI mass spectrum of fluoride species derived from reaction of $(i\text{-Bu})_7(C_6H_5CH{=}CH_2)$ T_8 and TMAF.[27a]

Similarly, Figure 3b shows a complex signal pattern when pure OPS and OVS are mixed in the presence of stoichiometric TMAF in THF. In this instance, no pure F^- encapsulated compounds are detected. Bowers et al. suggest that the broad multiplet between ~ -81 and ~ -83 ppm represents a complex mixture of compounds resulting from cage scrambling.[27a]

The ESI mass spectrum (Figure 4) observed from the reaction of $(i\text{-Bu})_7(C_6H_5CH{=}CH_2)$ T_8 and TMAF provides further evidence for F^--mediated cage rearrangements.[27] The spectrum shows peaks corresponding to $F^-@(i\text{-Bu})_6\text{Styrl}_2$, $F^-@(i\text{-Bu})_5\text{Styrl}_3$, and $F^-@(i\text{-Bu})_4\text{Styrl}_4$ T_8 side products in addition to the target $F^-@(i\text{-Bu})_7\text{Styrl}$ T_8 cage. The presence of additional side products having mixed functionalities can only be reasonably explained by the complex scrambling of the original starting material catalyzed by F^-.

The reactivity of $F^-@(RSiO_{1.5})_8$ compounds, as illustrated in Figures 3 and 4, suggests dynamic F^--mediated rearrangements of the silsesquioxanes in solution. It is likely that the fluoride ion catalyzes the exchange of $RSiO_x$- groups among cages, perhaps also assisted by traces of water, as the authors report that scrambling is not observed in anhydrous THF.[27]

The work presented here seeks to take advantage of F^--mediated SQ rearrangements to synthesize multifunctional cage compounds with a statistically controlled distribution of functionalities. Judging from the observations reported by Bowers, Mabry, et al.,[27] we anticipated that the number and type of functional groups on the target molecule could be controlled statistically by manipulating the ratio of SQs prior to equilibration with F^-. The first step in demonstrating the potential of this approach was recently published.[34] In that work we reported the utility of F^- catalysis (as TBAF) to transform the insoluble "T" resins polyvinyl- and polymethyl-SQs into mixed vinyl/Me functional T_{10} and T_{12} cages.

In the current work, we successfully extend our approach to a new class of multifunctional compounds with one or two (or more) distinct functionalities that may later be modified through chemical synthesis. These functional cages in turn can serve as possible platforms for (1) thermally stable, linear, and soluble SQ polymers with the capability of being spin/spray/dip-coated, cast, drawn, etc.; (2) low-T_m, alkylated SQ polymers for high-temperature lubrication applications, as was previously demonstrated for OPS;[11b] and (3) SQ polymers functionalized with liquid crystalline (LC) mesogens for the fabrication of unique LC polymeric materials, etc.[11c]

The synthesis of the SQ oligomers described below is meant to be representative of the unique potential F^--catalyzed exchange offers to produce mixed-functional SQs. It also provides a first example of the development of di- and trifunctional SQs that can be oligomerized to form "beads on a chain" (BoC) compounds. A further objective in these studies was to produce BoCs that are potentially fully conjugated. The impetus here was to determine if conjugated BoC oligomers might also offer 3-D interactions in the excited state,[33,35] as reported in a previous paper[35] and an accompanying paper.[33] On the basis of this previous work, we anticipated that we would observe an exceptional red-shift in emission behavior compared with that of model compounds that do not have the potential to exhibit cage−cage interactions in the excited state.

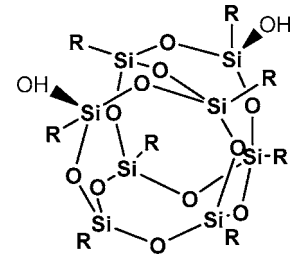

Figure 5. Disilanol silsesquioxane monomer (R = c-C_6H_{11}).[38]

Reactive monofunctional silsesquioxanes are typically used as copolymerizable pendant groups for traditional polymer systems.[36,37] They are readily prepared from "corner capping" reactions of partially condensed trisilanol cages and monofunctional trichlorosilanes. Relatively few polymers with cages along the chain backbone have been reported, however, because known routes to reactive difunctional cage compounds are rare and/or inefficient. For example, the polymerizable disilanol cage of Figure 5 is synthesized in only 15% yield after 12 weeks.[38]

PolyphenylSQ (PPS) and polyvinylSQ (PVS) are attractive precursors for fluoride-mediated rearrangement reactions as they were expected to provide access to functionalized SQ *cages* originating from generally "useless" polymeric starting materials. PPS is a byproduct in the synthesis of OPS, formed in 5−20% yield from the 60 h reaction of phenyltriethoxysilane, 7.5 wt % KOH, and 10 wt % H_2O in refluxing toluene.[39] It has the general formula $(C_6H_5SiO_{1.5})_n$ and is reported to contain a mixture of linear chain, open-caged, and/or ladder-like structures.[40] In these studies, "n" $\approx$ 15 for PPS (determined by GPC analysis).

Similarly, PVS is formed as a byproduct in the synthesis of OVS, obtained from the hydrolysis of vinyltriethoxysilane in ethanol/H_2O solution.[41] PVS is formed as a methanol-insoluble byproduct in 60−70% yield. While the structure of PVS has not yet been studied in detail, it is assumed to have the fully condensed general formula $(C_2H_3SiO_{1.5})_n$ with some residual EtO- groups, as no νOH bands are seen in the FTIR spectrum.

2. Experimental Section

2.1. Analytical. NMR Analyses. All ^1H and ^{13}C NMR samples used $CDCl_3$ or DMSO, and the spectra were recorded on a Varian INOVA 400 spectrometer. ^1H NMR spectra were collected at 400

(35) Sulaiman, S.; Bhaskar, A.; Zhang, J.; Guda, R.; Goodson, T., III; Laine, R. M. *Chem. Mater.* **2008**, *20*, 5563.
(36) Lichtenhan, J. D. *Comments Inorg. Chem.* **1995**, *17*, 115.
(37) Lichtenhan, J. D. In *Polymeric Material Encyclopedia, Vol. 10*; Salamone, J. D., Ed.; CRC Press: New York, 1996; pp 7768−7778.
(38) (a) Lichtenhan, J. D.; Vu, N. Q.; Carter, J. A.; Gilman, J. W.; Feher, F. J. *Macromolecules* **1993**, *26*, 2141. (b) Haddad, T. S.; Lichtenhan, J. D. *J. Inorg. Organomet. Polym.* **1995**, *5*, 237.
(39) Kim, S.-G.; Sulaiman, S.; Fargier, D.; Laine, R. M. In *Materials Syntheses: A Practical Guide*; Shubert, U., Hüsing, N., Laine, R. M., Eds.; Springer: New York, 2008; pp 179−191.

MHz using a 6000 Hz spectral width, a relaxation delay of 3.5 s, a pulse width of 38°, 30k data points, and $CDCl_3$ (7.27 ppm) or DMSO-d_6 (2.50 ppm) as an internal reference. ^{13}C NMR spectra were collected at 100 MHz using a 25 000 Hz spectral width, a relaxation delay of 1.5 s, 75k data points, a pulse width of 40°, and $CDCl_3$ (77.23 ppm) or DMSO-d_6 (39.5 ppm) as the internal reference.

Thermal Gravimetric Analyses. Thermal stabilities of materials under N_2 or air were examined using a 2960 simultaneous DTA-TGA instrument (TA Instruments, Inc., New Castle, DE). Samples (5−10 mg) were loaded in alumina pans and ramped to 1000 °C while heating at 10 °C/min. The N_2 or air flow rate was 60 mL/min.

Differential Scanning Calorimetry. DSC was performed using a DSC 2910 calorimeter (TA Instruments, Inc.). The N_2 flow rate was 60 mL/min. Samples (10−15 mg) were placed in pans without capping and ramped to 400 °C (5 °C/min).

Fourier-Transform Infrared Spectroscopy. Diffuse reflectance infrared Fourier transform (DRIFT) spectra were recorded on a Nicolet 6700 series FTIR spectrometer (Thermo Fisher Scientific, Inc., Madison, WI). Optical-grade, random cuttings of KBr (International Crystal Laboratories, Garfield, NJ) were ground with 1.0 wt % of the sample to be analyzed. For DRIFT analysis, samples were packed firmly and leveled off at the upper edge to provide a smooth surface. The FTIR sample chamber was flushed continuously with N_2 prior to data acquisition in the range 4000−400 cm^{-1}.

Gel Permeation Chromatography. GPC analyses were done on a Waters 440 system equipped with Waters Styragel columns (7.8 × 300, HT 0.5, 2, 3, 4) with RI detection using an Optilab DSP interferometric refractometer and THF as solvent. The system was calibrated using polystyrene standards and toluene as reference. Analyses were performed using PL Caliber 7.04 software (Polymer Laboratories, Shropshire, UK).

Matrix-Assisted Laser Desorption/Ionization Time-of-Flight Spectrometry. MALDI-TOF analysis was done on a Micromass TofSpec-2E instrument equipped with a 337 nm nitrogen laser in positive-ion reflection mode using poly(ethylene glycol) as the calibration standard, 1,8,9-anthracenetriol (dithranol) as matrix, and $AgNO_3$ as ion source. Samples were prepared by mixing solutions of 5 parts dithranol (10 mg/mL in THF), 5 parts sample (1 mg/mL in THF), and 1 part $AgNO_3$ (10 mg/mL in water) and blotting the mixture on the target plate.

X-ray Diffraction Analysis. XRD was performed on a Rigaku rotating anode goniometer (Rigaku Denki., Ltd., Tokyo, Japan). The powder sample was packed on a glass specimen holder. XRD scans were made from 10° to 60° 2θ, using a scan rate of 2° min^{-1} in 0.05° increments and Cu Kα radiation (1.542 Å) operating at 40 kV and 100 mA. The Jade program (version 3.1 from Materials Data, Inc., Livermore CA) was used to determine the presence of any crystallographic phases.

UV−Vis Spectrometry. UV−vis spectra were recorded on a Shimadzu UV-1601 UV−vis transmission spectrometer. Samples were dissolved in THF and diluted to a concentration (10^{-3}−10^{-4} M) where the absorption maximum was <10% for a 1 cm path length.

Photoluminescence Spectrometry. Photoluminescence spectra were recorded on a Fluoromax-2 fluorimeter in THF using 320 nm excitation. Samples from UV−vis spectroscopy were diluted (10^{-5}−10^{-6} M) to avoid excimer formation and fluorimeter detector saturation.

2.2. Materials. PPS and PVS were synthesized using previously described methods.[34,39] A first-generation Grubbs's catalyst [$RuCl_2$(=CHPh)(PCy_3)$_2$], 1.0 M TBAF (∼5 wt % H_2O) in THF, and vinyltriethoxysilane were purchased from Aldrich and used as received. All other solvents were purchased from Fisher or Aldrich and used as received. All work was performed under N_2.

2.3. Synthesis Procedures. Synthesis of Vinyl$_x$Ph (x = 9, 11) T_{10} and T_{12} Silsesquioxanes. PPS (1.00 g, 7.7 mmol) and PVS (7.0 g, 88.5 mmol) were placed in a dry 250 mL round-bottom flask equipped with a magnetic stirrer and condenser. The flask was evacuated and flushed three times with N_2. THF (100 mL) and 0.96 mL (1.0 M in THF, 0.96 mmol) of 95% TBAF were added via syringe. The reaction mixture was stirred at room temperature for 48 h. $CaCl_2$ (0.8 g, 7.2 mmol) was added to the reaction mixture and stirred an additional 2 h. The insolubles (∼1 g) were then gravity filtered, and the solvent was removed under reduced pressure. The solid residue was dissolved in ∼15 mL of THF and precipitated into 300 mL of MeOH. The precipitated products were collected and dried *in vacuo* to give a white powder (7.05 g, 88% with respect to total initial mass of reactants). ^1H NMR (400 MHz, $CDCl_3$): δ 5.6−6.2 (br, −C*H*=CH_2), 6.9 (br, Ar−*H*), 7.4 (br, Ar−*H*), 7.6 (br, Ar−*H*). ^{13}C NMR: δ 126.9 (Ar−*C*), 130.2 (−Si−*C*H=CH_2), 130.7 (Ar−*C*), 139.8 (Ar−*C*), 136.0 (CH=*C*H_2). MALDI-TOF: m/z (Ag^+ adduct) = 899 [$AgSi_{10}O_{15}(C_2H_3)_{10}$], 949 [$AgSi_{10}O_{15}(C_2H_3)_9(C_6H_5)_1$], 999 [$AgSi_{10}O_{15}(C_2H_3)_8(C_6H_5)_2$], 1057 [$AgSi_{12}O_{18}(C_2H_3)_{12}$], 1107 [$AgSi_{12}O_{18}(C_2H_3)_{11}(C_6H_5)_1$], 1157 [$AgSi_{12}O_{18}(C_2H_3)_{10}(C_6H_5)_2$] amu. GPC (found): M_n = 1026, M_w = 1077, PDI = 1.05 (see also Table 6, below).

Synthesis of VinylPh$_x$ (x = 9, 11) T_{10} and T_{12} Silsesquioxanes. PPS (15.0 g, 116 mmol) and PVS (1.0 g, 12.6 mmol) were placed in a dry 250-mL round-bottom flask equipped with a magnetic stirrer and condenser. The flask was evacuated and flushed three times with N_2. THF (100 mL) and 1.29 mL (1.0 M in THF, 1.29 mmol) of 95% TBAF were added via syringe. The reaction mixture was stirred at room temperature for 48 h. $CaCl_2$ (0.8 g, 7.2 mmol) was added to the reaction mixture and stirred an additional 2 h. The insolubles (∼5 g) were then gravity filtered, and the solvent was removed under reduced pressure. The solid residue was dissolved in ∼15 mL of THF and precipitated into 300 mL of MeOH. The precipitated products were collected and dried *in vacuo* to give a white powder (11.52 g, 72% with respect to total initial mass of reactants). ^1H NMR (400 MHz, $CDCl_3$): δ 5.8−6.1 (br, −C*H*=CH_2), 7.1−7.8 (br, Ar−*H*). ^{13}C NMR: δ 127.0 (Ar−*C*), 130.0 (−Si−*C*H=CH_2), 130.6 (Ar−*C*), 134.0 (Ar−*C*), 136.1 (−CH=*C*H_2) ppm. MALDI-TOF: m/z (Ag^+ adduct) = 1141 [$AgSi_8O_{12}(C_6H_5)_8$], 1299 [$AgSi_{10}O_{15}(C_2H_3)_2(C_6H_5)_8$], 1349 [$AgSi_{10}O_{15}(C_2H_3)_1(C_6H_5)_9$], 1399 [$AgSi_{10}O_{15}(C_6H_5)_{10}$], 1557 [$AgSi_{12}O_{18}(C_2H_3)_2(C_6H_5)_{10}$], 1607 [$AgSi_{12}O_{18}(C_2H_3)_1(C_6H_5)_{11}$], 1658 [$AgSi_{12}O_{18}(C_6H_5)_{12}$] amu. GPC (found): M_n = 725, M_w = 754, PDI = 1.04 (see also Table 6).

Synthesis of Vinyl$_2$Ph$_x$ (x = 8, 10) T_{10} and T_{12} Silsesquioxanes. PPS (7.24 g, 56.0 mmol) and PVS (1.0 g, 12.6 mmol) were placed in a dry 250 mL round-bottom flask equipped with a magnetic stirrer and condenser. The flask was evacuated and flushed three times with N_2. THF (100 mL) and 0.69 mL (1.0 M in THF, 0.69 mmol) of 95% TBAF were added via syringe. The reaction mixture was stirred at room temperature for 48 h. $CaCl_2$ (0.8 g, 7.2 mmol) was added to the reaction mixture and stirred an additional 2 h. Insolubles (∼3 g) were then gravity filtered, and the solvent was removed under reduced pressure. The solid residue was dissolved in ∼15 mL of THF and precipitated into 300 mL of MeOH. The precipitated products were collected and dried *in vacuo* to give a white powder (6.67 g, 81% with respect to total initial mass of reactants). The products were further purified by column chromatography (silica, 1:10 THF/hexane), followed by TLC. ^1H NMR (400 MHz, $CDCl_3$): δ 5.2−6.3 (br, −C*H*=CH_2), 6.6−8.1 (br, Ar−*H*). ^{13}C NMR: δ 127.0 (Ar−*C*), 130.0 (−Si−*C*H=CH_2), 130.7 (Ar−*C*), 133.8 (Ar−*C*), 136.3 (−CH=*C*H_2). IR: 3066−2917 (νC=H), 1591(νC=C, Ar ring), 1429(νC=C, Ar ring), 1132

(40) (a) Laine, R. M.; Youngdahl, K. A.; Babonneau, F.; Hoppe, M. L.; Zhang, Z.-F.; Harrod, J. F. *Chem. Mater.* **1990**, *2*, 464. (b) Laine, R. M.; Rahn, J. A.; Youngdahl, K. A.; Harrod, J. F. In *Homogeneous Transition Metal Catalyzed Reactions*; Moser, W. R., Slocum, D. W., Eds.; ACS: Washington DC, 1992; p 553. (c) Tsumura, M.; Kiyoshi, A.; Kotani, J.; Hiraishi, M.; Iwahara, T. *Macromolecules* **1998**, *31*, 2716. (d) Lee, E.-C.; Kimura, Y. *Polym. J.* **1998**, *30*, 234. (e) Lee, E.-C.; Kimura, Y. *Polym. J.* **1998**, *30*, 730.

(41) Harrison, P. G.; Hall, C. *Main Group Metal Chem.* **1997**, *20*, 515.

(νSi−O), 729 (νSi−C) cm^{-1}. MALDI-TOF: *m*/*z* (Ag^+ adduct) = 1199 [$AgSi_{10}O_{15}(C_2H_3)_4(C_6H_5)_6$], 1249 [$AgSi_{10}O_{15}(C_2H_3)_3(C_6H_5)_7$], 1299 [$AgSi_{10}O_{15}(C_2H_3)_2(C_6H_5)_8$], 1349 [$AgSi_{10}O_{15}(C_2H_3)_1(C_6H_5)_9$], 1399 [$AgSi_{10}O_{15}(C_6H_5)_{10}$], 1458 [$AgSi_{12}O_{18}(C_2H_3)_4(C_6H_5)_8$], 1507 [$AgSi_{12}O_{18}(C_2H_3)_3(C_6H_5)_9$], 1557 [$AgSi_{12}O_{18}(C_2H_3)_2(C_6H_5)_{10}$] amu. GPC (found): M_n = 986, M_w = 1005, PDI = 1.02 (see also Table 6). TGA (air, 1000 °C): found 49.4%; $T_{d5\%}$ = 459 °C (see also Table 7).

Metathesis Reaction of Vinyl$_2$Ph$_x$ (x = 8, 10) T$_{10}$ and T$_{12}$ Silsesquioxanes and 4-Bromostyrene. Vinyl$_2$Ph$_x$ (x = 8, 10) T$_{10}$ and T$_{12}$ SQs (1.00 g) and 52 mg of first-generation Grubbs's catalyst[42] (0.13 mmol) were added to a dry 50 mL Schlenk flask under N_2. Dry CH_2Cl_2 (20 mL) was added by syringe, followed by 4-bromostyrene (2.48 mL, 19.0 mmol). The mixture was stirred at ambient for 72 h and then quenched by precipitation into 300 mL of MeOH. The solution was filtered, and the solids removed by filtration (0.98 g) were purified by column chromatography (silica, 1.5:8.5 THF/hexane), followed by TLC. ^{1}H NMR (400 MHz, $CDCl_3$): δ 5.2−6.1 (br, −C*H*=C*H*), 6.5−8.0 (br, Ar−*H*). ^{13}C NMR: δ 121.9 (−*C*−Br), 126.5 (Ar−*C*), 127.0 (Ar−*C*), 130.8 (−Si−*C*H=CH−), 131.9 (Ar−*C*), 132.0 (Ar−*C*), 134.0 (Ar−*C*), 136.0 (−Si−CH=*C*H−). IR: 3079−2958 (νC=H), 1593 (νC=C, Ar ring), 1429 (νC=C, Ar ring), 1132 (νSi−O), 731 (νSi−C) cm^{-1}. MALDI-TOF: *m*/*z* (Ag^+ adduct) = 1399 [$AgSi_{10}O_{15}(C_6H_5)_{10}$], 1505 [$AgSi_{10}O_{15}(C_8H_6Br)_1(C_6H_5)_9$], 1610 [$AgSi_{10}O_{15}(C_8H_6Br)_2(C_6H_5)_8$], 1763 [$AgSi_{12}O_{18}(C_8H_6Br)_1(C_6H_5)_{11}$], 1867 [$AgSi_{12}O_{18}(C_8H_6Br)_2(C_6H_5)_{10}$] amu. GPC (found): M_n = 1383, M_w = 1437, PDI = 1.04 (see Table 6). TGA (air, 1000 °C): found 40.1%; $T_{d5\%}$ = 303 °C (see also Table 7).

Self-Metathesis Reaction of Vinyl$_2$Ph$_x$ (x = 8, 10) T$_{10}$ and T$_{12}$ SQs. Vinyl$_2$Ph$_x$ (x = 8, 10) T$_{10}$ and T$_{12}$ silsesquioxanes (1.00 g) and 52 mg of first-generation Grubbs's catalyst[42] (0.13 mmol) were added to a dry 50 mL Schlenk flask under N_2. Dry CH_2Cl_2 (20 mL) was added by syringe. The mixture was stirred at room temperature for 72 h and then quenched by precipitation into 300 mL of MeOH. The solution was filtered, and the recovered solid was analyzed by GPC, TGA, and MALDI, which confirmed only the presence of unreacted starting materials [vinyl$_2$Ph$_x$ (x = 8, 10) T$_{10}$ and T$_{12}$ SQs].

Heck Reaction of BrStyr$_2$Ph$_x$(x = 8, 10) T$_{10}$ and T$_{12}$ SQs and Vinyl$_2$Ph$_x$ (x = 8, 10) T$_{10}$ and T$_{12}$ Silsesquioxanes. To a dry 50 mL Schlenk flask under N_2 were added 0.50 g of BrStyr$_2$Ph$_x$ (x = 8, 10) T$_{10}$ and T$_{12}$, 19 mg (0.04 mmol) of Pd[P(*t*-Bu$_3$)]$_2$, and 18 mg (0.02 mmol) of $Pd_2(dba)_3$. 1,4-Dioxane (10 mL) was then added by syringe, followed by NCy_2Me (2.11 mmol, 0.45 mL) and 0.40 g of vinyl$_2$Ph$_x$ (x = 8, 10) T$_{10}$ and T$_{12}$. The mixture was stirred at room temperature for 72 h and then filtered through 1 cm Celite, which was washed with 5 mL of THF. The solution was then quenched by precipitation into 300 mL of methanol and filtered, and the solid redissolved was in 10 mL of THF. This solution was then filtered again through a 1 cm Celite column to remove any remaining Pd particles and reprecipitated into 200 mL of methanol. The products were further purified by column chromatography (silica, 1:10 THF/hexane), followed by TLC, collected, and dried *in vacuo* to give a white powder (0.72 g). ^{1}H NMR (400 MHz, $CDCl_3$): δ 5.1−6.3 (br, −C*H*=C*H*), 6.5−7.9 (br, Ar−*H*). ^{13}C NMR: δ 127.3 (Ar−*C*), 129.0−132.0 (Ar−*C*), 134.0 (Ar−*C*). IR: 3077−2979 (νC=H), 1591 (νC=C, Ar ring), 1429 (νC=C, Ar ring,), 1132 (νSi−O), 731 (νSi−C) cm^{-1}. MALDI-TOF: *m*/*z* (Ag^+ adduct) = 1399 [$AgSi_{10}O_{15}(C_6H_5)_{10}$], 1505 [$AgSi_{10}O_{15}(C_8H_6Br)_1(C_6H_5)_9$], 1763 [$AgSi_{12}O_{18}C_8H_6Br)_2(C_6H_5)_{10}$], 2593, 2697, 2797, 2849, 3003 amu. GPC (found): M_n = 2973, M_w = 3716, PDI = 1.25 (see also Table 6). TGA (air, 1000 °C): found 45.0%; $T_{d5\%}$ = 325 °C (see also Table 7).

Heck Reaction of BrStyr$_2$Ph$_x$ (x = 8, 10) T$_{10}$ and T$_{12}$ SQs and Vinyltriethoxysilane. To a dry 50 mL Schlenk flask under N_2 were added 0.50 g of BrStyr$_2$Ph$_x$ (x = 8, 10) T$_{10}$ and T$_{12}$, 19 mg (0.04 mmol) of Pd[P(*t*-Bu$_3$)]$_2$, and 18 mg (0.02 mmol) of $Pd_2(dba)_3$. 1,4-Dioxane (10 mL) was then added by syringe, followed by NCy_2Me (2.11 mmol, 0.45 mL) and 0.38 mL (2 mmol) of vinyltriethoxysilane. The mixture was stirred at room temperature for 72 h and then filtered through 1 cm Celite, which was washed with 5 mL of THF. The solution was then quenched by precipitation into 300 mL of methanol and filtered, and the solid was redissolved in 10 mL of THF. This solution was then filtered again through a 1 cm Celite column to remove any remaining Pd particles and reprecipitated into 200 mL of methanol. The products were further purified by column chromatography (silica, 1:10 THF/hexane), followed by TLC, collected, and dried *in vacuo* to give a white powder (0.58 g). ^{1}H NMR (400 MHz, $CDCl_3$): δ 1.2 (s, 3.6 H, −C*H*$_3$), 1.3 (s, 5.4 H, −C*H*$_3$), 3.8 (s, 2.4 H, −OC*H*$_2$CH$_3$), 3.9 (s, 3.6 H, −OC*H*$_2$CH$_3$), 5.1−6.3 (br, 4 H, −C*H*dbd*H*), 6.4−7.9 (br, 68 H, Ar−*H*). ^{13}C NMR: δ 18.0 (−*C*H$_3$), 58.8 (−O*C*H$_2$CH$_3$), 127.3 (Ar−C), 129.0−132.0 (Ar−*C*), 134.1 (Ar−*C*), 136.1 (−CH=CH). IR: 3087−2985 (νC=H), 2981−2811 (νC−H), 1591 (νC=C, Ar ring), 1431 (νC=C, Ar ring), 1132 (νSi−O), 737 (νSi−C) cm^{-1}. MALDI-TOF: *m*/*z* (Ag^+ adduct) = 1399 [$AgSi_{10}O_{15}(C_6H_5)_{10}$], 1614 [$AgSi_{10}O_{15}(C_6H_5)_9(C_{16}H_{23}O_3Si)_1$], 1828 [$AgSi_{10}O_{15}(C_6H_5)_8(C_{16}H_{23}O_3Si)_2$], 1872 [$AgSi_{10}O_{15}(C_6H_5)_{11}(C_{16}H_{23}O_3Si)_1$], 2086 [$AgSi_{10}O_{15}(C_6H_5)_{10}(C_{16}H_{23}O_3Si)_2$] amu. GPC (found): M_n = 1441, M_w = 1527, PDI = 1.06 (see also Table 6). TGA (air, 1000 °C): found 40.5%; $T_{d5\%}$ = 351 °C (see also Table 7).

3. Results and Discussion

Bassindale et al. unexpectedly discovered the presence of a trapped fluoride ion in the center of SQ cages in their efforts to improve SQ synthetic yields from alkoxysilanes using excess TBAF as base.[18,25] Bowers, Mabry, et al. incorporated F^- into SQs to increase the ionization efficiency of SQ-containing oligomers and polymers for mass spectrometry studies.[27] Though it is known that polyhedral SQs are easily observed by MALDI-TOF MS, high-molecular-weight SQ-containing polymers are not readily ionizable.[27] Bowers previously reported that MALDI characterization of two silsesquioxane oligomer systems (based on propylmethacrylates and siloxanes) were weakly detected and observed only for a maximum of three linked cages.[27] We also experienced similar difficulties detecting SQ oligomers by MALDI as described below.

Bowers et al. anticipated that incorporating F^- into SQ-containing polymers would increase their ionization efficiencies (or reduce the mass to charge ratio of the ions), making them easier to detect by MALDI-TOF MS. The coincidental F^--promoted scrambling serves as the inspiration for the work reported here.

Below we describe a simple and direct route to SQ BoC oligomers beginning with the reaction of catalytic amounts of TBAF with stoichiometrically controlled amounts of PPS and PVS, followed by $CaCl_2$ workup to capture F^- (Scheme 2). Failure to capture F^- after cage synthesis leads to further rearrangement and to mixed phenyl/vinyl resins of uncharacterizable products following solvent removal.[34] Subsequent chemical modification of the vinyl groups by alkene metathesis (see below) and Heck coupling leads to BoC SQ oligomers. As can be seen in Figures 6−8 (below), fluoride-ion-promoted rearrangement of PPS and PVS gives mixtures predominantly of the T$_{10}$ and T$_{12}$ cages, as described further below.

3.1. Synthesis of Vinyl$_x$Ph (x = 9, 11) T$_{10}$ and T$_{12}$ Silsesquioxanes. In efforts to synthesize cages having ~2 phenyl groups (with vinyl groups as the remaining moieties), a 10:1 mol ratio of PVS:PPS was reacted with 1 mol % TBAF in THF (room temperature/48 h; Scheme 2a). A minimum amount of TBAF was used to reduce the chance of residual F^- catalyzing unwanted side products during workup. An 8−10 mol % excess

(42) Grubbs, R. H. In *Handbook of Metathesis*; Wiley-VCH: New York, 2003.

Scheme 2. Fluoride-Mediated Rearrangement of PPS and PVS to (a) $Vinyl_xPh$ ($x = 9, 11$) T_{10} and T_{12} and (b) $Vinyl_2Ph_x$ ($x = 8, 10$) T_{10} and T_{12} Silsesquioxanes[a]

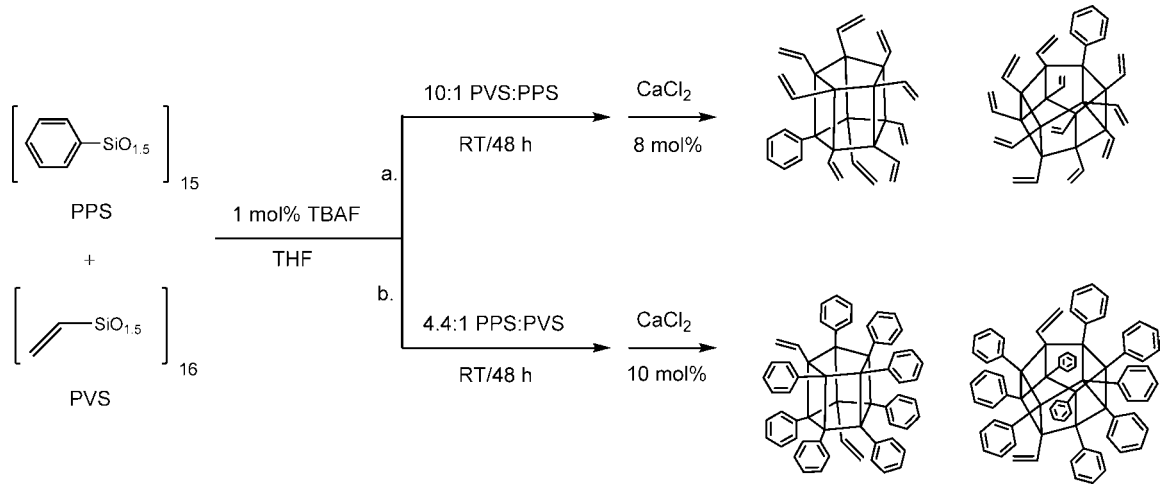

[a] The structures represent a mixture of isomeric substituents and not specific isomers.

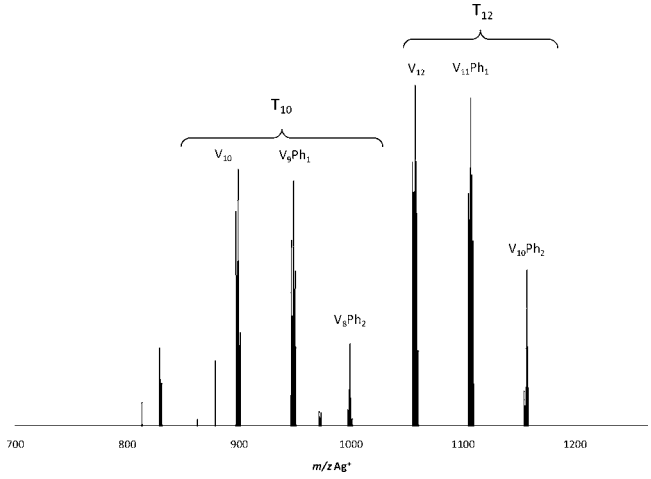

Figure 6. MALDI-TOF spectrum of 10:1 PVS:PPS reaction (THF) with catalytic TBAF (room temperature/48 h). The major products detected are the deca-/dodecavinyl and monophenylvinyl T_{10} and T_{12} cages.

Table 1. MALDI-TOF Data (Ag^+ Adduct) for 10:1 PVS:PPS Reaction with TBAF

compound formula	found (Da)	calcd (Da)	relative peak intensity
$(CH_2{=}CH)_{10}(SiO_{1.5})_{10}$	898.8	899.2	77
$(CH_2{=}CH)_9(C_6H_5)(SiO_{1.5})_{10}$	948.8	949.2	73
$(CH_2{=}CH)_8(C_6H_5)_2(SiO_{1.5})_{10}$	998.8	999.3	28
$(CH_2{=}CH)_{12}(SiO_{1.5})_{12}$	1056.9	1057.4	100
$(CH_2{=}CH)_{11}(C_6H_5)(SiO_{1.5})_{12}$	1106.9	1107.5	97
$(CH_2{=}CH)_{10}(C_6H_5)_2(SiO_{1.5})_{12}$	1156.9	1157.5	49

of $CaCl_2$ was used to trap F^- after completion of the reaction. Ca^{2+} reacts with F^- to form the insoluble CaF_2 salt, allowing for easy removal of fluoride ion from the products. Similarly, Cl^- reacts to form insoluble tetrabutylammonium chloride. The successful trapping of fluoride ion by $CaCl_2$ workup was confirmed by an absence of peaks in the ^{19}F NMR spectrum. The products were noncrystalline, as XRD powder patterns exhibited only amorphous scattering.

Figure 6 provides a MALDI-TOF spectrum of the 10:1 PVS:PPS reaction products. The most common isotopes are listed in Table 1. Small discrepancies (<1 Da) between "found" and "calculated" values listed in Table 1 may be due to ionization potential differences in the experimental environment or possibly errors in calibration. The MALDI spectrum in Figure 6 shows that the reaction does not give single T_8 products, as anticipated, but rather mixtures of T_{10} and T_{12} cages, with the dominant ionizable species being the unsubstituted deca- and dodecavinylsilsesquioxanes and monophenyl compounds. While MALDI indicates the presence of the intended diphenyl T_{10} and T_{12} compounds, no T_8 cubes are observed under these reaction conditions, perhaps indicating a preferential, thermodynamically controlled reaction pathway to T_{10} and T_{12} cages. Unlabeled peaks in Figure 6 correspond to fragments generated by the MALDI laser, mainly from loss of 1−2 vinyl ($-CH{=}CH_2$) groups from the T_{10} cages.

It is important to note that the *absolute* quantities of T_8, T_{10}, and T_{12} in the product mixture cannot be determined by MALDI alone because the distribution patterns are not perfectly quantitative. It is well-known that the peak heights in MALDI-TOF MS correspond to the ionization efficiencies of the species and are not necessarily representative of the amount of each in the sample. However, since SQ monomers are readily ionizable and many have been successfully characterized by MALDI techniques by us[11,33–35] and others,[27] we can use the MALDI peak heights as a relative (qualitative) measure of the amounts of each species in the monomeric sample.

Mono- and diphenylvinyl T_{10} and T_{12} compounds are potentially useful as thermally stable, high-density cross-linking agents or as platforms to 3-D "star"-type materials.[11,33–35] Furthermore, the synthesis of such compounds demonstrates the ability to tailor the numbers and types of functional groups on the SQ cages by simply altering the ratio of the polymeric starting materials. This capability is further demonstrated below in the synthesis of the related divinylphenyl T_{10} and T_{12} SQs, which serve as the starting materials for both cross-metathesis and Heck coupling, leading to the BoC oligomers described further below.

3.2. Synthesis of $Vinyl_2Ph_x$ ($x = 8, 10$) T_{10} and T_{12} Silsesquioxanes. A 10:1 mol ratio of PPS:PVS was reacted with 1 mol % TBAF in THF (room temperature/48 h) and gave results analogous to those found for the 10:1 PVS:PPS reaction, with monovinyl compounds being the major products according to MALDI-TOF MS (see Figure 7 and Table 2). MALDI also detects the presence of T_8 cubes in addition to the T_{10} and T_{12} species.

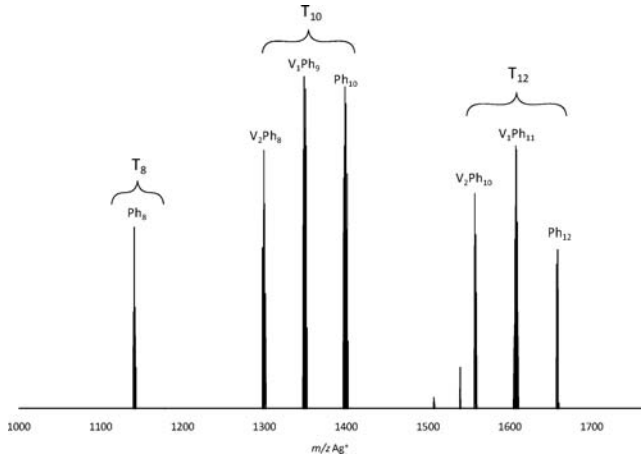

Figure 7. MALDI-TOF spectrum of 10:1 PPS:PVS reaction (THF) with catalytic TBAF (room temperature/48 h).

Table 2. MALDI-TOF Data (Ag^+ Adduct) for 10:1 PPS:PVS Reaction with TBAF

compound formula	found (Da)	calcd (Da)	relative peak intensity
$(C_6H_5)_8(SiO_{1.5})_8$	1141.1	1141.4	60
$(CH_2{=}CH)_2(C_6H_5)_8(SiO_{1.5})_{10}$	1299.2	1299.6	80
$(CH_2{=}CH)(C_6H_5)_9(SiO_{1.5})_{10}$	1349.2	1349.7	100
$(C_6H_5)_{10}(SiO_{1.5})_{10}$	1399.2	1399.8	97
$(CH_2{=}CH)_2(C_6H_5)_{10}(SiO_{1.5})_{12}$	1557.2	1558.0	68
$(CH_2{=}CH)(C_6H_5)_{11}(SiO_{1.5})_{12}$	1607.3	1608.1	81
$(C_6H_5)_{12}(SiO_{1.5})_{12}$	1658.3	1658.1	55

The MALDI spectrum in Figure 7 also shows the presence of OPS, decaphenyl- (dPS), and dodecaphenylSQs (DPS) species as byproducts of the synthesis. Divinyl compounds of the T_{10} and T_{12} cages are also observed.

Monovinyl silsesquioxane compounds offer potential use as organic−inorganic hybrid monomers for polymerization reactions and/or in the preparation of block copolymers, for example.[15,19,37,38] They can be also used as pendant or end-cap groups in existing polymer systems. Polymer resins incorporating thermally robust SQs can exhibit improved thermal stabilities (increased degradation temperatures), suggested to be associated with the heat capacity of the cage components, which form a glassy layer of SiO_xC_y during pyrolysis that retards diffusion of O_2 through the surface char.[36]

Alternatively, others suggest that increased thermal stability is achieved by retarding polymer chain motion, either by intermolecular interactions (between the cages and polymer chains) or by the tendency of the large cage molecules to restrict the mobility of the polymer segments at elevated temperatures.[43] Fu et al. reported that pendant cubes also enhance the mechanical properties of polymers, such as the tensile strength of styrene−butadiene−styrene triblock copolymers near the T_g of styrene.[44] Those authors speculated that the pendant cubes act as "physical cross-linkers" in these systems and provide sites for physical constraint opposing the viscous flow of polymer chains at higher temperatures, which is responsible for the improved load-carrying capacity over polymers that do not contain cubes.[44]

After trial and error, we found that reaction of a 4.4:1 mol ratio of PPS:PVS with TBAF in THF (room temperature/48 h; Scheme 2b) gave predominantly the T_{10} and T_{12} divinyl compounds, as shown by the MALDI spectrum in Figure 8. Divinyl compounds are particularly important because further reaction of the two vinyl moieties can lead to BoC oligomers/polymers, as explained below.

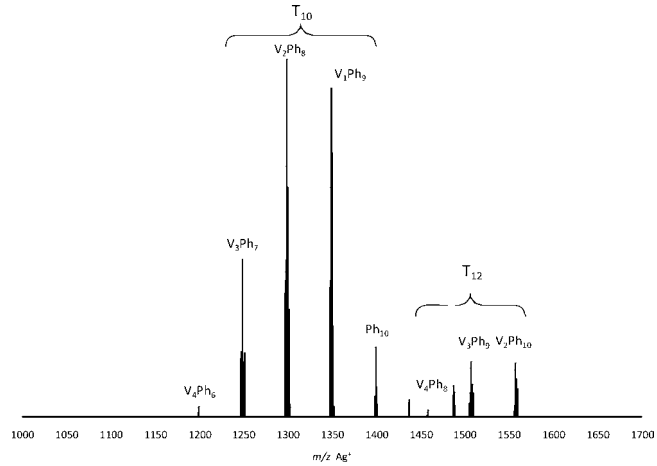

Figure 8. MALDI-TOF spectrum of 4.4:1 PPS:PVS reaction with TBAF (room temperature/48 h) after purification by column chromatography.

Table 3. MALDI-TOF Data (Ag^+ Adduct) for 4.4:1 PPS:PVS Reaction with TBAF

compound formula	found (Da)	calcd (Da)	relative peak intensity
$(CH_2{=}CH)_4(C_6H_5)_6(SiO_{1.5})_{10}$	1199.1	1199.5	12
$(CH_2{=}CH)_3(C_6H_5)_7(SiO_{1.5})_{10}$	1249.4	1249.6	49
$(CH_2{=}CH)_2(C_6H_5)_8(SiO_{1.5})_{10}$	1299.8	1299.6	100
$(CH_2{=}CH)(C_6H_5)_9(SiO_{1.5})_{10}$	1349.3	1349.7	93
$(C_6H_5)_{10}(SiO_{1.5})_{10}$	1399.8	1399.8	27
$(CH_2{=}CH)_4(C_6H_5)_8(SiO_{1.5})_{12}$	1458.0	1457.9	17
$(CH_2{=}CH)_3(C_6H_5)_9(SiO_{1.5})_{12}$	1507.8	1508.0	23
$(CH_2{=}CH)_2(C_6H_5)_{10}(SiO_{1.5})_{12}$	1557.9	1558.0	23

The 4.4:1 PPS:PVS reaction MALDI-TOF spectrum shows reaction products corresponding to Ag^+ adducts of T_{10} and T_{12} cages; see Table 3. A small amount of phenyl T_8 cube formed as a byproduct and is easily removed by column chromatography for reasons discussed below. MALDI indicates the presence of mono- and divinylphenyl T_{10} and T_{12} as well as small amounts of tri- and tetravinyl T_{10} and T_{12}. The structures of the T_{10} and T_{12} products are supported by FTIR, ^{1}H NMR, and ^{13}C NMR data, as listed below. XRD powder patterns exhibit only amorphous scattering.

The dominant ionizable species according to the MALDI-TOF spectrum in Figure 8 is the $vinyl_2Ph_8T_{10}$ species, as anticipated. Separation (and thus quantification) of the cage species resulting from the reaction of 4.4:1 PPS:PVS by column chromatography is not trivial due to similarities in the chemical structures and properties (e.g., solubility, polarity, etc.) of the products.

The progress of the reaction of a 4.4:1 mol ratio of PPS:PVS with 1 mol % TBAF was monitored by GPC, as shown in Figure 9. At the beginning ($t = 0$ h), only one broad peak appears for PPS and PVS [retention time (t_R) $\approx$ 31.5 min]. After 1 h, a large peak corresponding to the T_{10} and T_{12} cages appears ($t_R \approx 33$ min; see also Figure 13, below), indicating that the reaction proceeds rapidly on catalyst addition. At $t = 2$ h, the PPS peak height drops to ~54% of the peak height at $t = 1$ h, indicating further rearrangement.

Unreacted PPS is consumed more slowly as the reaction stirs longer than ~2 h. The unreacted PPS peak height drops an

(43) Liu, Y. R.; Huang, Y. D.; Liu, L. *Polym. Degrad. Stab.* **2006**, *91*, 2731.
(44) Fu, B. X.; Lee, A.; Haddad, T. S. *Macromolecules* **2004**, *37*, 5211.

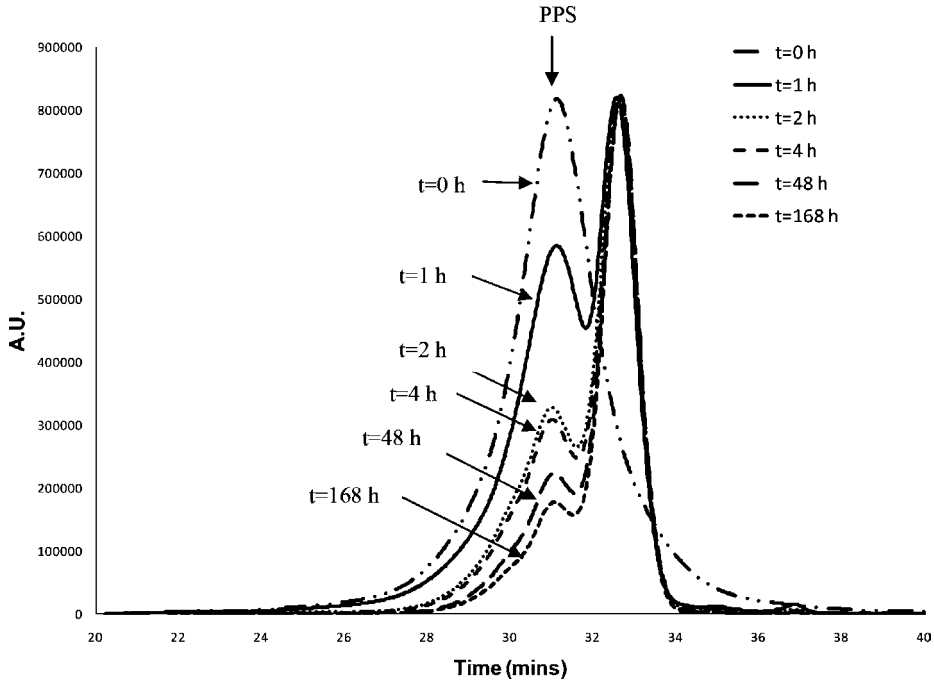

Figure 9. Progress of 4.4:1 PPS:PVS mole ratio reaction catalyzed by 1 mol % TBAF, monitored by GPC.

Scheme 3. Alkene Metathesis of $Vinyl_2Ph_x$ (x = 8, 10) T_{10} and T_{12} SQs with 4-Bromostyrene

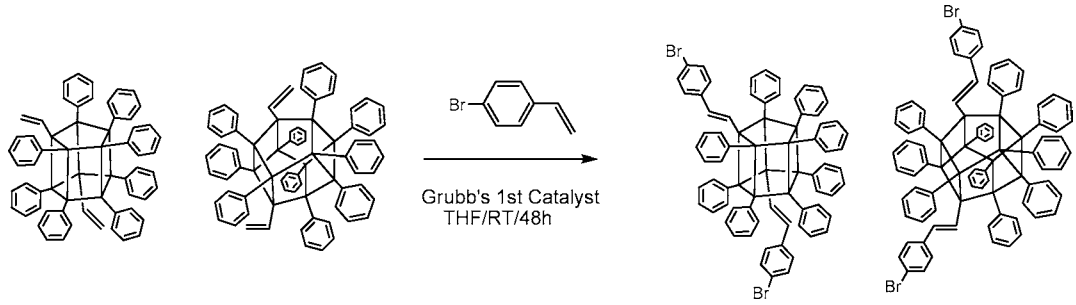

additional 22% over 5 d (from t = 48 to 168 h), as opposed to 54% over 1 h (t = 1−2 h) at the beginning of the reaction. Thus, the reaction seems to reach equilibrium after 48 h, giving an 81% yield of divinyl cage products with respect to mass of initial reactants. We could not accurately determine a rate law, as PPS is only sparingly soluble in THF.

Unreacted PPS is collected as insoluble material after $CaCl_2$ workup or separated from the products by column chromatography (see Experimental Section). While the rearrangement reactions work well using 1 mol % TBAF, it may be possible to improve the reaction times/yields by using more catalyst or increasing the reaction temperature. A detailed study of the effects of catalyst amounts (and/or temperature) on the reaction rate is needed and remains an area for further study.

The TGA behavior and a more detailed characterization of the GPC trace of these materials are discussed below in comparison with all the products made here.

3.3. Metathesis of $Vinyl_2Ph_x$ (x = 8, 10) T_{10} and T_{12} SQs and 4-Bromostyrene. $Vinyl_2Ph_x$ (x = 8, 10) T_{10} and T_{12} (from reaction of 4.4:1 PPS:PVS with TBAF) were reacted with 4-bromostyrene per Scheme 3. MALDI MS of the crude metathesis products initially showed the presence of $BrStyr_3T_{10}$ and T_{12} as well as $BrStyr_4$ T_{10} and T_{12} compounds, indicating reaction of the trivinyl and tetravinyl cages present in the starting material (Figure 8). However, the bromostyrenyl compounds are more easily purified by column chromatography than the corresponding vinyl precursors, as the $BrStyr_3$ and $BrStyr_4$ derivatives are much more soluble than the mono-BrStyr and $BrStyr_2$ derivatives. However, it proved difficult to completely remove phenyl T_{10} even after column chromatography because of its high solubility.[22]

Table 4. MALDI-TOF Data (Ag^+ Adduct) for Metathesis Reaction of $Vinyl_2Ph_x$ (x = 8,10) T_{10} and T_{12} and 4-Bromostyrene

compound formula	found (Da)	calcd (Da)	relative peak intensity
$(C_6H_5)_{10}(SiO_{1.5})_{10}$	1399.1	1399.8	100
$(C_8H_6Br)(C_6H_5)_9(SiO_{1.5})_{10}$	1503.5	1504.7	18
$(C_8H_6Br)_2(C_6H_5)_8(SiO_{1.5})_{10}$	1610.0	1609.6	74
$(C_8H_6Br)(C_6H_5)_{11}(SiO_{1.5})_{12}$	1763.1	1763.1	19
$(C_8H_6Br)_2(C_6H_5)_{10}(SiO_{1.5})_{12}$	1867.0	1868.0	50

Thus, after column chromatography, MALDI-TOF of the purified metathesis products indicated that all of the vinyl groups react to give ∼2 aryl bromides per T_{10} and T_{12} as sites for further functionalization; see Table 4 and Figure S1 in Supporting Information. Low-intensity signals from the monobromostyrenyl (BrStyr) T_{10} and T_{12} were also present in the spectrum.

The ^1H NMR spectrum of the purified metathesis products was complex, and the broad peaks corresponding to the vinyl and phenyl protons from varying amounts of different compounds were not useful for determining the structures of the

Scheme 4. Attempted Olefin Self-Metathesis of $Vinyl_2Ph_x$ ($x = 8, 10$) T_{10} and T_{12} SQs

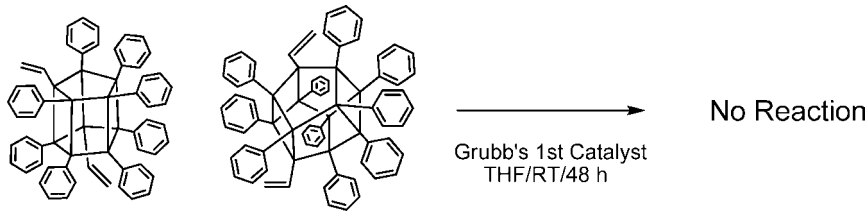

Scheme 5. Heck Coupling of $Vinyl_2Ph_x$ T_{10}/T_{12} SQs with $BrStyr_2Ph_x$ T_{10}/T_{12} SQs ($x = 8, 10$)

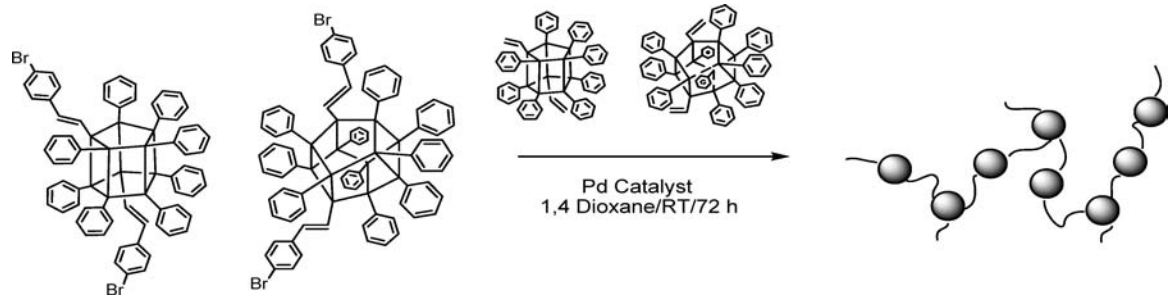

products. ^{13}C NMR, however, shows distinct peaks for the vinyl carbons at ~130.8 (−Si−*C*H═CH−) and ~136.0 (−Si−CH═*C*H−) ppm. Peaks were assigned by comparison to ^{13}C NMR spectra of vinyltriethoxysilane and phenyltriethoxysilane.[45] A peak at ~122 ppm is characteristic of bromine bonded to an aryl carbon, associated with the bromostyrenyl moieties of the expected product. The generally weak aromatic νC−Br stretch (~1028−1073 cm^{-1}) was not observed in the FTIR, possibly due to overlap with the very intense and broad νSi−O−Si peak (~1130 cm^{-1}) characteristically associated with SQ cages. As above, the TGA and GPC data are discussed below.

A self-metathesis reaction of the divinyl cages using the same reaction conditions was attempted (Scheme 4) in efforts to directly synthesize cage oligomers/polymers. This resulted only in recovery of the starting materials (as determined by GPC, MALDI TOF, and TGA), likely due to the steric effects of the bulky phenyl groups and/or cages impeding formation of the intermediate four-member ring in the cross-metathesis mechanism.[46] This suggests that cages with longer, more flexible vinyl-terminated tethers and/or less bulky nonreactive moieties may be more amenable to metathetical self-coupling. Furthermore, a molecular diluent with two reactive vinyl groups could be used to link the bulky cages together, for example. Reactions such as these also remain an area for further study.

3.4. Heck Reaction of $BrStyr_2Ph_x$ ($x = 8, 10$) T_{10}/T_{12} SQs and $Vinyl_2Ph_x$ ($x = 8, 10$) T_{10}/T_{12} SQs. $BrStyr_2Ph_x$ ($x = 8, 10$) T_{10} and T_{12} silsesquioxanes were reacted with $vinyl_2Ph_x$ ($x = 8, 10$) T_{10} and T_{12} under Heck coupling conditions (Scheme 5) in efforts to form BoC oligomers. The isolated products are soluble in typical organic solvents (THF, ethyl acetate, and acetone), with proposed structures shown schematically in Figure 10.

Table 5. MALDI-TOF Data (Ag^+ Adduct) for Heck Reaction of $BrStyr_2Ph_x$ ($x = 8, 10$) T_{10} and T_{12} and $Vinyl_2Ph_x$ ($x = 8, 10$) T_{10} and T_{12}

compound formula	found (Da)	calcd (Da)	relative peak intensity
$(C_6H_5)_{10}(SiO_{1.5})_{10}$	1400.0	1399.8	100
$(C_8H_6Br)(C_6H_5)_9(SiO_{1.5})_{10}$	1505.1	1504.7	20
$(C_8H_6Br)(C_6H_5)_{11}(SiO_{1.5})_{12}$	1763.2	1763.1	39

Table 5 shows the relevant MALDI data after Heck coupling (see also Figure S2 in the Supporting Information). Unreacted monobromostyrenyl species are present in the spectrum, as are unreactive phenyl T_{10}, which could not be completely separated from the starting materials by column chromatography. Higher molecular weight species (from dimers, trimers, etc.) are not readily detected by MALDI, because of the difficulties in ionizing SQ oligomers/polymers.[27] ESI MS was also attempted but gave results similar to those obtained withh MALDI and did not show the presence of high-molecular-weight species.

Figure 11 records the GPC traces for $[vinylSiO_{1.5}]_8$ (OVS) and $[PhSiO_{1.5}]_8$ (OPS), as well as the F^--equilibrated products, the metathesis products, the model compounds (see below), and finally the BoC Heck coupling products. OVS and OPS are included as standards for comparison of separation and retention

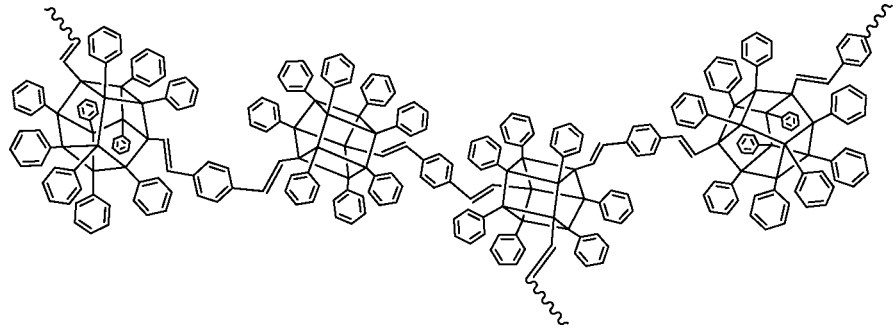

Figure 10. General BoC structure of Heck coupling product.

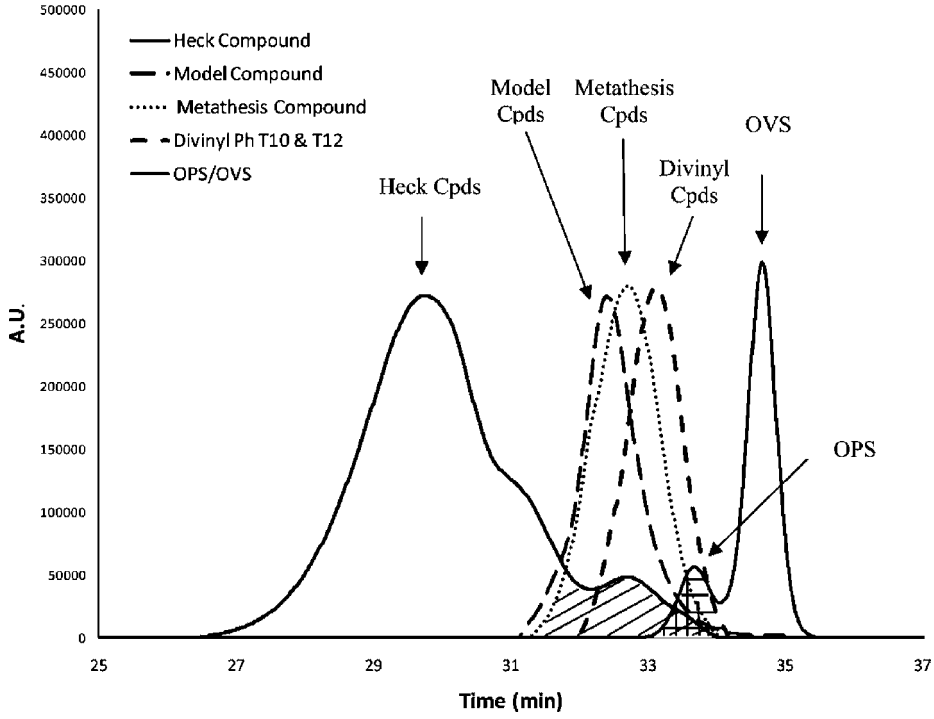

Figure 11. GPC trace of Heck, model, and metathesis compounds, vinyl$_2$Ph$_8$ T_{10}, vinyl$_2$Ph$_{10}$ T_{12}, and OPS/OVS (for comparison). Shaded areas represent amounts of unreacted starting materials in divinyl, metathesis, and Heck compounds (~5%, ~4%, and ~10%, respectively).

Table 6. GPC Mass Data for Heck, Model, and Metathesis Compounds, Vinyl$_2$Ph$_8$ T_{10}, Vinyl$_2$Ph$_{10}$ T_{12}, and OPS/OVS (for Comparison)

compound formula	t_R (min)	M_n	M_w	PDI
Heck compounds[a]	29.7	2973	3716	1.25
model compounds	32.3	1441	1527	1.06
metathesis compounds	32.6	1383	1437	1.04
divinyl Ph T_{10} and T_{12}	33.1	986	1005	1.02
OPS	33.7			
OVS	34.6			

[a] Area under curve measured from t_R = 26.4 to 31.9 min.

times. Table 6 compiles the pertinent information gleaned from the Figure 11 data.

The GPC data provide a wealth of information. For example, the amount of $[PhSiO_{1.5}]_{10}$ in the product mixture can be estimated to be <5% by GPC. This is calculated by comparing the area of overlap between the divinyl T_{10} and T_{12} peak and phenyl T_8 peak. As previously suggested, GPC cannot adequately resolve phenyl T_8, T_{10}, or T_{12} due to similarities in their hydrodynamic volumes. Comparing the area of overlap with phenyl T_8 gives a rough estimate of the amount of unreacted phenyl T_{10} in the product mixture. This estimate is supported by the TGA data below.

The GPC trace of the metathesis products shows a single, narrow peak (PDI = 1.04; see Table 6), confirming the absence of polymeric side products and retention of intact silica cores. There is a small difference in the retention times of the peaks corresponding to the metathesis compounds and vinyl$_2$Ph T_{10} and T_{12}, owing to only a slight increase in the hydrodynamic volumes after metathesis with 4-bromostyrene.

A slight shoulder in the GPC at $t_R \approx 31$ min most likely indicates formation of dimerized cages. Unreacted BrStyrT_{10} and T_{12} also appear as a small peak ($t_R \approx 32$ min). The total amount of unreacted BrStyrT_{10} and T_{12} and phenyl T_{10} is ~10% by GPC.

The BoC Heck coupling products appear in the GPC at t_R = 26−31 min with a PDI of 1.25. The MW of these materials suggests that the degree of polymerization runs 2−5. Figure 10 portrays an idealized BoC structure. However, it is likely that these structures are not linear but branched or highly branched, leading to an underestimation of the true MWs. Thus, on the conservative side, we suggest that at most these molecules are trimeric or tetrameric in nature.

The TGAs of the various products in air and N_2 are shown in Figures S3 and S4, respectively, in the Supporting Information. The TGAs of the vinyl$_2$Ph$_x$ (x = 8, 10) T_{10} and T_{12} compounds indicate that they are very stable in air ($T_{d5\%}$ = 460 °C; Table 7), as expected of SQ cages containing rigid, thermally stable phenyl groups. The mass loss before 500 °C may be due to sublimation of phenyl T_{10} (~5 wt %), corroborating the GPC-estimated amount of this compound.

The ceramic yields of the divinyl Ph T_{10} and T_{12} products are 49.4%. An accurate theoretical ceramic yield could not be calculated because the products are a mixture of different cage structures of unknown quantities. However, a comparison of the ceramic yield to the theoretical ceramic yields of the individual compounds in the mixture (as detected by MALDI) corresponds closely (±4%, neglecting the amount of phenyl T_{10}) as evidenced in Table 7.

The $T_{d5\%}$ of the metathesis compounds is ≈ 300 °C (Table 7). The ceramic yields of the metathesis products (40.1%) correspond closely to the range (39.9−43.6%) of theoretical ceramic yields of the compounds in the mixture. The $T_{d5\%}$ for the Heck product is 325 °C indicating that these oligomers are very thermally stable in air yet highly soluble (and therefore processable). The ceramic yield of the Heck compounds is 45.0%. An accurate determination of the theoretical ceramic

(45) SDBS Spectral Database, http://riodb01.ibase.aist.go.jp/sdbs/cgi-bin/ENTRANCE.cgi (accessed May 15, 2009).
(46) Grubbs, R. H. *Prog. Inorg. Chem.* **1978**, *24*, 1.

Table 7. Decomposition Temperatures ($T_{d5\%}$) and Ceramic Yields for Heck, Model, and Metathesis Compounds, $Vinyl_2Ph_8T_{10}$ and $Vinyl_2Ph_{10}T_{12}$[a]

compound	$T_{d5\%}$ (°C)	ceramic yield (%)	theor ceramic yield (%)
Heck compounds	325	45.0	
model compounds	351	40.5	
$(C_8H_6Br)(C_6H_5)_9(SiO_{1.5})_{10}$			39.9
$(C_8H_6Br)_2(C_6H_5)_8(SiO_{1.5})_{10}$			35.0
$(C_8H_6Br)(C_6H_5)_{11}(SiO_{1.5})_{12}$			40.9
$(C_8H_6Br)_2(C_6H_5)_{10}(SiO_{1.5})_{12}$			36.5
$(C_6H_5)_{10}(SiO_{1.5})_{10}$			30.3
metathesis compounds	303	40.1	
$(C_8H_6Br)(C_6H_5)_9(SiO_{1.5})_{10}$			43.0
$(C_8H_6Br)_2(C_6H_5)_8(SiO_{1.5})_{10}$			39.9
$(C_8H_6Br)(C_6H_5)_{11}(SiO_{1.5})_{12}$			43.6
$(C_8H_6Br)_2(C_6H_5)_{10}(SiO_{1.5})_{12}$			41.0
$(C_6H_5)_{10}(SiO_{1.5})_{10}$			30.3
divinyl Ph T_{10} and T_{12}	459	49.4	
$(CH_2{=}CH)_3(C_6H_5)_7(SiO_{1.5})_{10}$			52.7
$(CH_2{=}CH)_2(C_6H_5)_8(SiO_{1.5})_{10}$			50.4
$(CH_2{=}CH)(C_6H_5)_9(SiO_{1.5})_{10}$			48.4
$(CH_2{=}CH)_4(C_6H_5)_8(SiO_{1.5})_{12}$			53.4
$(CH_2{=}CH)_3(C_6H_5)_9(SiO_{1.5})_{12}$			51.5
$(CH_2{=}CH)_2(C_6H_5)_{10}(SiO_{1.5})_{12}$			49.7
$(C_6H_5)_{12}(SiO_{1.5})_{12}$			30.3

[a] Conditions: air, 10°C/min to 1000 °C. Theoretical ceramic yields for compounds detected by MALDI are given for reference.

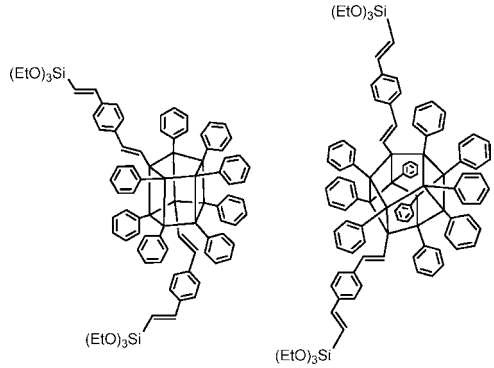

Figure 12. Structures of Heck model compounds from reaction of $BrStyr_2Ph_x$ (x = 8, 10) T_{10} and T_{12} SQs with vinyltriethoxysilane.

yields is impossible since the products are an oligomeric mixture of different cage compounds.

3.5. Synthesis of Model Compounds by Heck Reaction of $BrStyr_2Ph_x$ (x = 8, 10) T_{10} and T_{12} SQs and Vinyltriethoxysilane. We prepared the model compounds shown in Figure 12 via reaction of $BrStyr_2Ph_x$ (x = 8, 10) T_{10} and T_{12} SQs with vinyltriethoxysilane [$CH_2{=}CH{-}Si(OEt)_3$] under Heck conditions (see below). The goal here was to compare their UV−vis absorption and emission data with those of the Heck products (Figure 10), as discussed below.

The MALDI spectrum of the model compounds after purification by column chromatography is shown in Figure 13, and the correct masses for the disubstituted Ag^+ adducts are observed at m/z 1828 [$(C_{16}H_{23}O_3Si)_2Ph_8$ T_{10}] and 2086 [$(C_{16}H_{23}O_3Si)_2Ph_{10}$ T_{12}] amu (see also Table 8). The MALDI spectrum also shows peaks corresponding to the monosubstituted T_{10} and T_{12} cages, as well as decaphenyl SQ present as an impurity in the starting materials. GPC shows a single, narrow peak at $t_R \approx 32.3$ min (PDI = 1.06; Figure 11 and Table 6).

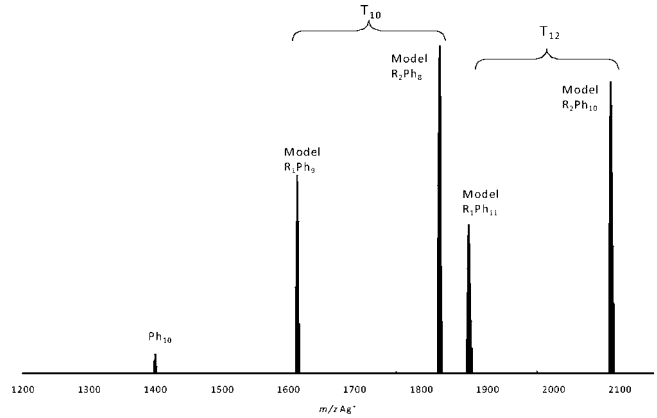

Figure 13. MALDI-TOF spectrum after Heck reaction of $BrStyr_2Ph_x$ (x = 8, 10) T_{10} and T_{12} SQs and vinyltriethoxysilane, purified by column chromatography.

Table 8. MALDI-TOF Data (Ag^+ Adduct) for Heck Reaction of Model Compounds

compound formula	found (Da)	calcd (Da)	relative peak intensity
$(C_6H_5)_{10}(SiO_{1.5})_{10}$	1399.1	1399.8	7
$(C_6H_5)_9(C_{16}H_{23}O_3Si)(SiO_{1.5})_{10}$	1614.0	1614.1	61
$(C_6H_5)_8(C_{16}H_{23}O_3Si)_2(SiO_{1.5})_{10}$	1827.9	1828.4	100
$(C_6H_5)_{11}(C_{16}H_{23}O_3Si)(SiO_{1.5})_{12}$	1872.1	1872.5	46
$(C_6H_5)_{10}(C_{16}H_{23}O_3Si)_2(SiO_{1.5})_{12}$	2086.0	2086.8	89

The FTIR spectra are also consistent with the structures associated with the model compounds (see Experimental Section).

The $T_{d5\%}$ for the model compounds is 350 °C (Table 7). The small mass loss (∼5 wt %) before 500 °C as the model compounds are heated in N_2 (see Figure S4, Supporting Information) is attributed to sublimation of a small amount of phenyl T_{10}. The ceramic yield (40.5%) corresponds to the range (35.0−40.9%) of theoretical ceramic yields for compounds detected by MALDI in the product mixture.

The ^1H NMR spectrum of the model compounds (Figure S5, Supporting Information) exhibits broad peaks in the aromatic (∼6.4−7.9 ppm) and vinyl (∼5.1−6.3 ppm) proton regions that are typical for these compounds. Peaks at ∼3.8−3.9 and ∼1.2−1.3 ppm correspond to the $-OCH_2$ and $-CH_3$ protons, respectively. The theoretical ratio of vinyl:methoxy:methyl protons (1:1.5:2.3) matches the actual integration (1:1.4:2.3). There are two distinct signals for both the methoxy and methyl peaks, likely indicating protons in two magnetically different environments originating from the mono- and difunctional species and/or the T_{10} and T_{12} cages. Integration of the separate signals comprising the peaks for methoxy and methyl protons gives a ratio ∼1.5:1 for each. We can therefore assume that the T_{10} and T_{12} cages are present in similar proportions, though we cannot determine which cage species is present in the greater amount because the effect of the cage structure on the proton chemical shifts is unknown.

The ^{13}C NMR spectrum of the model compounds (Figure S6, Supporting Information) shows characteristic peaks for the methyl and methoxy carbons (∼18 and ∼59 ppm, respectively) and aryl carbons (∼127−134 ppm). Vinyl carbons are attributed to the peak at ∼136 ppm. Peaks were assigned by comparing with ^{13}C NMR spectra for vinyltriethoxysilane, phenyltriethoxysilane, and triphenylchlorosilane.[45]

3.6. UV−Vis Absorption and Emission Studies. As noted above, and in the accompanying paper, we find unusual red-

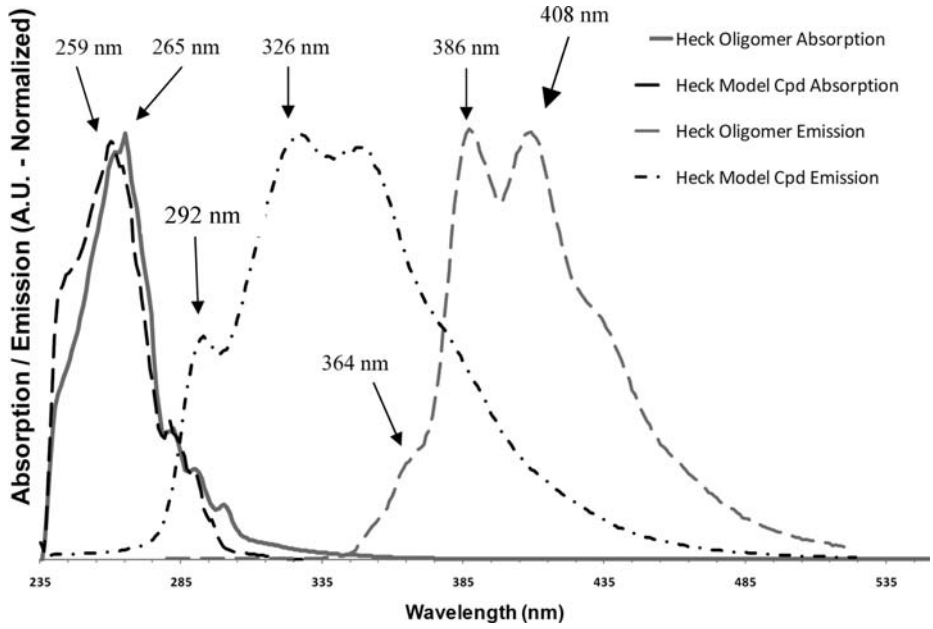

Figure 14. Solution (THF) absorption and emission spectra ($\lambda_{excitation} = 265$ nm) of Heck compounds and corresponding Heck model $-Si(OEt)_3$ compounds.

shifted emission spectra for octastilbene[33] and for octavinylstilbene[35] derivatives in first- and second-generation "star" compounds derived from OVS and $[p\text{-I-phenylSiO}_{1.5}]_8$ and $[o\text{-Br-phenylSiO}_{1.5}]_8$. These compounds exhibit highly red-shifted emissions typical of molecules with extensively delocalized electronic structures, which are unexpected in compounds that, to date, are thought of as silica-like insulators.

On the basis of our observations, we interpreted these results to suggest that organic moieties on the cage periphery interact electronically with the predicted, spherical LUMO located within the cage cores (see above).[35] If this is indeed the case, then all 8, 10, or even 12 functional groups on T_8, T_{10}, or T_{12} SQs may "communicate electronically" simultaneously through the cage in the excited state.

As noted in the Introduction, the synthesis of fully "conjugated" BoCs of the type shown in Scheme 5 appeared to be a method to test for this type of behavior both in larger SQs and also in oligomeric species. To ensure that we were actually measuring excited-state behavior involving several SQ cages linked via conjugated organic components, we also synthesized the above-described model compounds. The model T_{10} and T_{12} compounds were synthesized with end-caps of $-Si(OEt)_3$ intended to model the $Si(O-)_3$ vertices of the cages in the BoCs.

Thereafter, their UV−vis behavior in THF at high dilution (10^{-5}−10^{-6} M) was assessed per Figure 14. As can be seen, both the BoC and the model compounds absorb with essentially the same maximum absorption near 260 nm. However, the emission spectra are quite different.

As can be seen, the model compounds emit with maxima at 292, 326, and 340 nm, whereas the BoC system emits at 364, 386, and 408. The BoC oligomers are red-shifted ~60 nm from the model compounds alone. The Figure 14 spectra imply that addition of a cage to another cage using a conjugated tether increases conjugation and induces this shift.

Furthermore, the observed red-shift suggests delocalization in the excited state in the T_{10} and T_{12} cages in a manner similar to that observed in the T_8 SQs.[33,35,48,49] If there is indeed conjugation through the cage centers, the delocalization would be expected to lower the energy of the $\pi \rightarrow \pi^*$ transition and shift the emission maxima to longer wavelengths as a consequence.

These results are a compelling argument for the existence of a 3-D excited-state interaction through the cage centers and seem to agree with previous results from our group and corroboration of recent modeling studies in this area.[29–33,47–49] In addition, it seems reasonable to assume that the ease of fluoride encapsulation inside the cube core reflects the unique electronic characteristics of these molecules and thus may help explain their unexpected emission behavior. Further exploration of this phenomenon in detail is necessary and remains an area for further study.

4. Conclusions

Fluoride-mediated rearrangement reactions of silsesquioxanes allow direct access to a new class of multifunctional cage compounds, offering unique and viable possibilities to build statistically ordered, nanometer structures through simple control of the ratio of the beginning materials. The F^- rearrangement of polymeric phenyl- and vinylsilsesquioxanes, in particular, is exciting because the reactants are "useless" polymeric byproducts in common silsesquioxane syntheses and lead opportunely to product mixtures of discrete polyhedral silsesquioxane cages. Silsesquioxane cages with ~2 reactive functionalities may be further modified and tailored to synthesize high-molecular-weight linear polymers with silsesquioxanes directly incorporated along the chain backbone. These

(47) (a) Sellinger, A.; Tamaki, R.; Laine, R. M.; Ueno, K.; Tanabe, H.; Williams, E.; Jabbour, G. E. *Chem. Commun.* **2005**, 3700. (b) Lo, M. Y.; Zhen, C.; Lauters, M.; Jabbour, G. E.; Sellinger, A. *J. Am. Chem. Soc.* **2007**, *129*, 5808.

(48) Zhen, C.-G.; Becker, U.; Kieffer, J. *J. Phys. Chem. A* **2009**, *113*, 9707–9714.

(49) Takahashi, K.; Brick, C. M.; Sulaiman, S.; Laine, R. M., unpublished work.

polymers could offer unique and tunable properties, such as high thermal stability, improved mechanical properties, and liquid crystalline behavior. We illustrate the potential of these compounds here in the synthesis of novel, fluorescent "BoC" oligomers with high solubility and thermal stability (up to 325 °C). The highly red-shifted (∼60 nm) emission behavior of these compounds is unique in its own right, as it suggests extensive electron delocalization and may involve conjugation through the silsesquioxane cores. The chemistries explored here are representative of many diverse structures of varying complexity that can be created using these simple cages as molecular scaffolds.

Acknowledgment. We thank NSF for support of this work through grant CGE 0740108. We also thank the state of Michigan for partial support of this work through a MUCI grant.

Supporting Information Available: Detailed spectroscopic characterizations of the various compounds prepared in this work. This material is available free of charge via the Internet at http://pubs.acs.org.

JA9087743